Ultracold atomic Bose and Fermi spinor gases in optical lattices

You may also be interested in:

Anti-ferromagnetic spinor BECs in optical lattices
Davide Rossini, Matteo Rizzi, Gabriele De Chiara et al.

The physics of dipolar bosonic quantum gases
T Lahaye, C Menotti, L Santos et al.

Pseudospin and spin–spin interactions in ultracold alkali atoms
D H Santamore and E Timmermans

Non-standard Hubbard models in optical lattices: a review
Omjyoti Dutta, Mariusz Gajda, Philipp Hauke et al.

Recent developments in quantum Monte Carlo simulations with applications for cold gases
Lode Pollet

Cold and ultracold molecules: science, technology and applications
Lincoln D Carr, David DeMille, Roman V Krems et al.

Precision measurement of spin-dependent interaction strengths for spin-1 and spin-2 ^{87}Rb atoms
Artur Widera, Fabrice Gerbier, Simon Fölling et al.

Quantum dynamics, particle delocalization and instability of Mott states: the effect of fermion–boson conversion on Mott states
Fei Zhou and Congjun Wu

Exotic magnetic orders for high spin-ultracold fermions
E. Szirmai and M. Lewenstein

Ultracold atomic Bose and Fermi spinor gases in optical lattices

K Eckert[1,7]**, Ł Zawitkowski**[2]**, M J Leskinen**[3]**, A Sanpera**[1,4]
and M Lewenstein[4,5,6]

[1] Departament Física, Grup Física Teórica, Universitat Autònoma de Barcelona,
E-08193 Bellaterra, Spain
[2] Centrum Fizyki Teoretycznej, Polska Akademia Nauk, Warszawa,
02668 Poland
[3] Nanoscience Center, Department of Physics, PO Box 35,
University of Jyväskylä, Finland
[4] Institució Catalana de Recerca i Estudis Avançats (ICREA),
E-08010 Barcelona, Spain
[5] Institut de Ciències Fotòniques (ICFO), E-08860 Castelldefels,
Barcelona, Spain
[6] Institut für Theoretische Physik, Universität Hannover,
D-30167 Hannover, Germany
E-mail: kai@uab.es

Abstract. We investigate magnetic properties of Mott-insulating phases of ultracold Bose and Fermi spinor gases in optical lattices. We consider in particular the $F = 2$ Bose gas, and the $F = 3/2$ and $5/2$ Fermi gases. We derive effective spin Hamiltonians for one and two atoms per site and discuss the possibilities of manipulating the magnetic properties of the system using optical Feshbach resonances. We discuss low temperature quantum phases of a ^{87}Rb gas in the $F = 2$ hyperfine state, as well as possible realizations of high spin Fermi gases with either ^{6}Li or ^{132}Cs atoms in the $F = 3/2$ state, and with ^{173}Yb atoms in the $F = 5/2$ state.

[7] Author to whom any correspondence should be addressed.

IOP Institute of Physics **Φ** DEUTSCHE PHYSIKALISCHE GESELLSCHAFT

Contents

1. Introduction

1.1. Spinor Bose gases in optical lattices

The seminal theory papers by Ho [1], and Ohmi and Machida [2] on spinor $F = 1$ Bose–Einstein condensates (BECs) as well as the experiments performed by the MIT group on optically trapped $F = 1$ sodium condensates [3], have brought a new perspective to the study of magnetic systems

using ultracold atomic gases. Recent studies involving both $F = 1$ and $F = 2$ rubidium atoms have focused on the rich dynamics of spinor Bose condensates [4]–[7] (for theory see for instance [8]), as well as on exotic phases (as, for instance, nematic, half-vortices, and singlet superfluids (SFs)[8]). Ground-state (GS) and dynamical properties of $F = 3$ Bose condensates have also been discussed in connection to ongoing experiments with chromium atoms [10].

Experiments on bosonic spinor lattice gases, as they are planned by many groups [11], should open new avenues. Confining spinor BECs in optical lattices offers a unique opportunity to study magnetic properties of matter, as a large range of tunable parameters exists, which are not accessible in solid state systems (for a review see [12]). Spinor gases also offer novel possibilities of detection [13, 14], for the engineering of strongly correlated states, and for the processing of quantum information.

1.1.1. F = 1 gases in optical lattices. Intensive studies of $F = 1$ systems have already been carried out by Demler's and Zhou's groups [15]. Imambekov *et al* have derived an approximate phase diagram for the case of antiferromagnetic interactions of ^{23}Na. As in the standard Bose–Hubbard model, an $F = 1$ spinor gas undergoes SF to Mott insulator (MI) transition as tunnelling is decreased. In the antiferromagnetic case in two-dimensional (2D) and 3D systems, the SF phase is *polar*, and so are the Mott states with an odd number N of atoms per site (those states are also termed as *nematic*). In the case of even N, for small tunnelling the Mott states are singlets, and for moderate tunnelling there occurs a first-order transition to the nematic state.

For small tunelling, the system can be described via an effective spin model [15, 16]. Especially, this model for a single particle per site has the possibility of a dimerized state, as in the Majumdar–Ghosh model [17]. For ^{23}Na, the existence of a dimerized ground state is still under debate. Partially dimerized states were studied by Yip [16]. A variational ansatz interpolating between dimer and nematic states indicated that in a wide range of parameters the spinor ^{23}Na lattice gas should indeed have a partially dimerized GS in 1D, 2D, and 3D (see also [18]). Partially dimerized states are an interesting but controversial prediction, since so far such states have not been observed in experiments. Results not consistent with those of Yip have been found by Zhou [19]. He developed an effective nonlinear sigma model and pointed out the role of fully dimerized valence bond crystals (dVBC) in the $F = 1$ spin chain. For further studies of $F = 1$ systems using gauge models see [20, 21]. The existence of dimer ordering for ^{23}Na was recently confirmed by Rizzi *et al* [22], who studied numerically the SF–MI transition in the $F = 1$ Bose-Hubbard model in 1D. For a single particle per site, in the regime where the effective spin model works, according to their findings the system is always dimerized. Similar results were obtained by Porras *et al* [23]. Thus, strictly speaking, nematic order is absent in 1D in the thermodynamic limit. However, susceptibility to nematic ordering grows close to the border to the ferromagnetic phase, indicating that it may persist in finite systems.

1.1.2. F = 2 gases in optical lattices. The mean field states of spinor $F = 2$ gases were investigated for the first time in [24–27]. It is worth noticing that mean field results are also valid for MI states with one atom per lattice site, provided that all atoms are described by the same single-particle wave function attached to a given site. The authors of [25, 26] go one step further, and apart from the mean field theory consider also the extreme case of quenched (immobile)

---

[8] Free half-vortices play a particularly important role in 2D, where they drive the analogue of the Kosterlitz–Thouless transition, see [9].

$F = 2$ bosons in an optical lattice. In other words, these articles characterize possible on-site states for N bosons with total spin S in the absence of tunneling.

After submission of the first version of this paper, Barnett *et al*, presented a beautiful classification of the mean field phases for arbitrary F, based on the 19th century method by F Klein of solving quintic polynomials by the analysis of rotations of regular icosahedra [28]. We discuss their results in more detail in the following. Also, very recently the effective spin Hamiltonians (in the first MI lobe) and quantum insulating phases of $F = 2$ bosons have been studied by Zhou and Semenoff [29], applying the variational principle to product (Guztwiller ansatz, cf [30]), dimer, and trimer states. Their results concerning effective spin Hamiltonians agree with ours.

1.2. Spinor Fermi gases in optical lattices

Obviously, there is an enormous interest also in Fermi gases, and in particular in spinor Fermi gases in optical lattices. The first reason is, of course, that such systems could realize a perfect quantum simulator of the fermionic Hubbard model, and thus shine some light on the problem of high T_c superconductivity. For spin $F = 1/2$ this has been proposed in [31], and recently considered with three-component fermions in [32].

Liu *et al* [33] proposed to use fermions with high F to realize spin-dependent Hubbard models, in which hopping parameters are spin-dependent. Such models lead to exotic kinds of superfluidity, such as to a phase in which SF and normal components coexist at zero temperature. Hofstetter and collaborators have written a series of papers, reviewed in [34], on fermionic atoms with $SU(N)$ symmetry in optical lattices. Such systems also have exotic SF and flavour-ordered GSs, and exhibit very rich behaviour in the presence of disorder.

It is, of course, inevitable to ask which atoms can be used to realize high-F fermonic spinor gases in optical lattices. The most commonly used alkali ^{6}Li has hyperfine manifolds with $F = 1/2$ and $3/2$. The latter is, obviously, subjected to two-body losses, but as in the case of the $F = 2$ manifold of rubidium, one can expect reasonably long life time in the lattice (especially in MI states with $N = 1$). Another commonly used fermion is a heavy alkali ^{40}K, which has manifolds $F = 7/2$ and $9/2$. These fermions are particularly useful for spin-dependent Hubbard models [33].

There are several atoms whose lowest hyperfine manifold has $F = 3/2$, i.e. in those GSs two body losses can be avoided: ^{9}Be, ^{132}Cs, or ^{135}Ba, but so far only the bosonic caesium BEC has been achieved [35]. On the other hand, recently a BEC of ^{174}Yb atoms [36], as well as a degenerate gas of ^{173}Yb fermions with $F = 5/2$, has been realized. Finally, fermionic chromium has 4 hyperfine manifolds with $F = 9/2, 7/2, 5/2, 3/2$, in the ascending order of energies, and after achieving BEC of the bosonic chromium [37], the prospects for achieving ultracold degenerate Fermi gases are very good.

1.2.1. $F = 3/2$ and $5/2$ Fermi gases in optical lattices.

Recently, there has been a lot of progress in understanding the special properties of $F = 3/2$ and $5/2$ Fermi gases. In spin-3/2 systems with contact interaction, Wu *et al* realized that a generic $SO(5)$ symmetry exists [38]. They also found novel competing orders [39, 40], suggesting a quartetting phase and the *s*-wave quintet Cooper pairing phase.

Different results have been obtained from the bosonization approach applied to 1D systems with $F = 3/2, 5/2, \ldots$ by Lecheminant *et al* [41, 42]. They used a model with a spin-independent coupling U and a coupling in the singlet channel V (which is exact for $F = 3/2$,

but somewhat simplified for $F \geqslant 5/2$), and studied the phase diagram in the U–V plane. They found 3 phases: a spin density wave, an atomic density wave (which may crossover to a molecular SF), and a BCS (Bardeen–Cooper–Schrieffer) SF (that may crossover to a molecular density wave). They have also classified Mott phases at commensurate $1/(F + 1/2)$ fillings. Finally, the $F = 3/2$ model has been solved analytically using the Bethe ansatz [43]. An overview of hidden symmetries and competing orders in spin-3/2 gases is presented in the excellent paper by Wu [44].

1.2.2. Goals of the paper.   Concerning the Bose gases, the main goal of the present paper is to make predictions for the planned experiments with ultracold $F = 2$ ^{87}Rb atoms in the strongly correlated regime. We will thus concentrate on characterizing possible MI states in the limit of weak tunnelling. In this sense we will generalize the results of [25, 26]. We will disregard here the Zeeman effect by assuming sufficiently efficient magnetic shielding. Also, we will only consider the MI states with $N = 1$ or 2 atoms per site. Higher atom numbers will inevitably lead to 3-body losses, and will be thus much more difficult to realize experimentally.

We will also analyse the possibility of exploring parameters of the systems by modifying atomic scattering lengths. This cannot be done using the standard Feshbach resonances (cf [45]), since we assume zero magnetic field. Instead, one has to use the method of optical Feshbach resonances (OFR) proposed by Fedichev *et al* [46].

Our main goal will be to derive effective spin models in the experimentally relevant regimes, to study the GSs of the systems, and in particular to identify those instances when exact solutions are available, either in the form of product (mean field) states, or the so called matrix product states (MPS) [47], similarly as it happens in the famous AKLT model [48].

Similar goals concern Fermi gases, although there much less is known about values of scattering lengths, the possibility of OFR, etc. We will take our liberty here to explore larger regions of parameters, assuming optimistically that they will become feasible experimentally at some point.

This paper is addressed to both atomic physics and condensed matter audiences, and for this reason an extended version of the introduction can be found in [49].

1.2.3. Plan of the paper.   In section 2 we discuss the Bose–Hubbard Hamiltonian (BHH) of $F = 2$ bosons in an optical lattice and its GSs when atoms are quenched at fixed lattice sites. In section 3 we derive an effective spin Hamiltonian for this system. In section 4 we investigate which types of GSs could be achieved, assuming a (limited) experimental control over the spin-dependent scattering lengths. In sections 5 and 6 we analyse the Fermi–Hubbard and the effective Hamiltonian for $F = 3/2$, and in sections 7 and 8 we perform a similar analysis for $F = 5/2$. We conclude in section 9. Appendix B contains a detailed analysis of possibilities of optical manipulations of scattering lengths of ^{87}Rb atoms in the $F = 2$ hyperfine manifold. Appendix B gives a short overview of MPS and projected entangled pair states (PEPS) methods.

2. $F = 2$ Spinor Bose–Hubbard Hamiltonian

2.1. The system

We consider $F = 2$ atoms at low temperatures confined in a deep optical lattice so that the system is well described by a Bose–Hubbard Hamiltonian (BHH) [30]. We assume atoms to interact

via a zero-range potential. The total angular momentum of two colliding identical bosons is restricted to even values due to Bose symmetry, so that the s-wave interaction between two spin-2 particles can be written as $\hat{V} = \bar{g}_0 \hat{P}_0 + \bar{g}_2 \hat{P}_2 + \bar{g}_4 \hat{P}_4$, where $\hat{P}_S$ ($S = 0, 2, 4$) is the projector onto the subspace with total spin S. The interaction strengths, $\bar{g}_S$, depend on the total spin of the two colliding particles. For the different channels they are given by the scattering lengths a_S through $\bar{g}_S = 4\pi\hbar^2 a_S/m$.

To better understand GS properties of the Hamiltonian it is convenient to express the interaction potential $\hat{V}$ in terms of spin operators. Making use of the identities $\hat{I} = \hat{P}_0 + \hat{P}_2 + \hat{P}_4$ and $\hat{\mathbf{F}}_1 \cdot \hat{\mathbf{F}}_2 = -6\hat{P}_0 - 3\hat{P}_2 + 4\hat{P}_4$, where $\hat{\mathbf{F}}_i$ corresponds to the spin operator of particle i, we find $\hat{V} = \bar{c}_0 \hat{I} + \bar{c}_1 \hat{\mathbf{F}}_1 \cdot \hat{\mathbf{F}}_2 + \bar{c}_2 \hat{P}_0$. Here $\bar{c}_0 = (3\bar{g}_4 + 4\bar{g}_2)/7$, $\bar{c}_1 = (\bar{g}_4 - \bar{g}_2)/7$, and $\bar{c}_2 = (3\bar{g}_4 - 10\bar{g}_2 + 7\bar{g}_0)/7$ [25]. Following [26], $\hat{P}_0$ can also be expressed in terms of 'singlet pair' creation and annihilation operators $\hat{S}_+ = \hat{a}_0^\dagger \hat{a}_0^\dagger/2 - \hat{a}_1^\dagger \hat{a}_{-1}^\dagger + \hat{a}_2^\dagger \hat{a}_{-2}^\dagger$, $\hat{S}_- = \hat{S}_+^\dagger$, where $\hat{a}_\sigma^\dagger$ ($\hat{a}_\sigma$) creates (annihilates) a particle with spin projection σ. The operator $\hat{S}_+$ applied on the vacuum creates, except for normalization, two bosons in a spin singlet state. Such a pair does not represent a composite boson, as $\hat{S}_+$ and $\hat{S}_-$ do not satisfy Bose commutation relations. $\hat{P}_0 = 2\hat{S}_+ \hat{S}_-/5$. Its eigenvalues are $N_S(2N - 2N_S + 3)/5$, where the quantum number N_S denotes the number of spin-singlet pairs and N the total number of bosons [26].

2.2. Bose–Hubbard Hamiltonian

The 1D BHH for spin $F = 2$ can be written as

$$\hat{H} = -t \sum_{\langle ij \rangle, \sigma} (\hat{a}_{\sigma i}^\dagger \hat{a}_{\sigma j} + \hat{a}_{\sigma j}^\dagger \hat{a}_{\sigma i}) + \sum_{i,S} g_S \hat{P}_{Si}, \tag{1}$$

or alternatively

$$\hat{H} = -t \sum_{\langle ij \rangle, \sigma} (\hat{a}_{\sigma i}^\dagger \hat{a}_{\sigma j} + \hat{a}_{\sigma j}^\dagger \hat{a}_{\sigma i}) + \frac{c_0}{2} \sum_i \hat{N}_i (\hat{N}_i - 1) + \frac{c_1}{2} \sum_i : \hat{\mathbf{F}}_i \cdot \hat{\mathbf{F}}_i : + \frac{2c_2}{5} \sum_i \hat{S}_{+i} \hat{S}_{-i}, \tag{2}$$

where $\hat{a}_{\sigma i}$ annihilates a particle in a hyperfine state with $m_F = \sigma$ at site i, $\hat{N}_i = \sum_\sigma \hat{a}_{\sigma i}^\dagger \hat{a}_{\sigma i}$ is the number of particles at site i, $\hat{\mathbf{F}}_i = \sum_{\sigma\sigma'} \hat{a}_{\sigma i}^\dagger \mathbf{T}_{\sigma\sigma'} \hat{a}_{\sigma' i}$ is the spin operator at site i ($\mathbf{T}_{\sigma\sigma'}$ being the usual spin matrices for a spin-2 particle), and $: \hat{X} :$ denotes normal ordering of the operator $\hat{X}$. Interaction strengths $\bar{g}_s$ and the $\bar{c}_i$s are modified due to the orthogonal confinement, such that $g_S = \bar{g}_S [\int dy |w(y)|^4]^2$ and $c_i = \bar{c}_i [\int dy |w(y)|^4]^2$, where $w(y)$ is the Wannier function for the orthogonal direction centred at $x = 0$. The first two terms in the Hamiltonian represent tunnelling between nearest-neighbour sites and Hubbard repulsion between atoms on the same site, respectively, as in the standard Bose–Hubbard model. The two remaining terms represent the energy associated with spin configurations within lattice sites. The ratios between the various interactions, c_1/c_0 and c_2/c_0, are fixed by the scattering lengths ($c_1/c_0 = \bar{c}_1/\bar{c}_0$ and $c_2/c_0 = \bar{c}_2/\bar{c}_0$). We assume here that the scattering lengths are such that the Hamiltonian (2) is stable with respect to collapse. Stability requires the $g_S \geqslant 0$ for all S, which is the case, e.g. for ^{87}Rb. The ratio t/c_0 between tunnelling and Hubbard repulsion can be tuned by changing the lattice parameters [30]. When $t \ll c_0$, the system is in a Mott-insulating phase in which atoms are quenched at fixed lattice sites. We consider here the case when tunneling is sufficiently weak compared to Hubbard repulsion so that it can be treated as a perturbation with t/c_0 being a small parameter. We study systems with one and two particles per site, which are the most interesting cases as they do not suffer from three-body losses.

2.3. On-site Hamiltonian

To zeroth order, the Hamiltonian is a sum of independent single-site Hamiltonians (we omit the index i):

$$\hat{H}_0 = \frac{c_0}{2}\hat{N}(\hat{N}-1) + \frac{c_1}{2} : \hat{\mathbf{F}} \cdot \hat{\mathbf{F}} : + \frac{2c_2}{5}\hat{S}_+\hat{S}_-. \tag{3}$$

Exact eigenstates of this Hamiltonian have been obtained in [26]. Since $\hat{S}_{\pm}$ commute with the total spin operator, the energy eigenstates can be labeled with four quantum numbers as $|N, N_S, \bar{F}\rangle_{m_{\bar{F}}}$, where N is the number of particles per site, N_S the number of spin-singlet pairs, and $\bar{F}$ is the total on-site spin. The eigenstates have a $2\bar{F}+1$-fold degeneracy associated with the quantum number $m_{\bar{F}}$. Their energies are:

$$E = \frac{c_0}{2}N(N-1) + \frac{c_1}{2}(\bar{F}(\bar{F}+1) - 6N) + \frac{c_2}{5}N_S(2N - 2N_S + 3). \tag{4}$$

In general there is an additional degeneracy which, however, manifests itself only for states with larger number N of particles per site than considered in this paper. Single particle states correspond to $|1, 0, 2\rangle_{m_F} = \hat{a}^{\dagger}_{m_F}|\Omega\rangle$, being $|\Omega\rangle$ the vacuum. Explicit expressions for two and three particle states with maximal spin projection can be found in [26].

2.4. Phases at $t = 0$

It is easy to check which phases will be realized in the limit of vanishing tunneling for a given chemical potential. For $\mu < 0$ the state with no atoms has the smallest (Gibbs potential) energy $G = E - \mu N = 0$. For $\mu \geqslant 0$ we enter the phase with one atom for site $|1, 0, 2\rangle$ with $G = -\mu$. As we increase μ further, we enter into one of the phases with two atoms per site, namely the one that corresponds to the smallest g_S and $G = g_S - 2\mu$: (i) $|2, 1, 0\rangle$ if $g_0 \leqslant g_2, g_4$, (ii) $|2, 0, 2\rangle$ if $g_2 \leqslant g_0, g_4$, and (iii) $|2, 0, 4\rangle$ if $g_4 \leqslant g_2, g_0$.

3. Effective Hamiltonian for $F = 2$

To derive the effective Hamiltonian to second-order in t we consider the two-site problem. The tunnelling Hamiltonian $H_t = -t\sum_{\sigma,\langle ij\rangle}(\hat{a}^{\dagger}_{\sigma i}\hat{a}_{\sigma j} + \hat{a}^{\dagger}_{\sigma j}\hat{a}_{\sigma i})$ conserves both the total spin S and the projection of the total spin m_S [15]. Thus, to second-order, the shift of the energy of the two-site GS $|g, S\rangle$ with total spin S is given by

$$\epsilon_S = -\sum_{\nu} \frac{|\langle \nu|\hat{H}_t|g, S\rangle|^2}{E_{\nu} - E_{g,S}}, \tag{5}$$

where ν denotes the (virtual) intermediate states and E_{ν}, $E_{g,S}$ are the unperturbed energies of the two-site states $|\nu\rangle$, $|g, S\rangle$ (which are non-degenerate apart from the m_F degeneracy). The dependence of the energy shifts on the total spin of the two sites introduces nearest-neighbour spin–spin interactions in the lattice. It is sufficient to evaluate these shifts for only one value of the projection m_S of the total spin. This is because tunnelling cannot mix states with different m_S and overlaps $|\langle \nu|H_t|g, S\rangle|$ are rotationally invariant. To simplify the calculations we always choose the highest possible value of m_S.

3.1. One atom per site

3.1.1. Pair Hamiltonian. For a single particle per site, i.e. $|1, 0, 2\rangle^{(i)} \otimes |1, 0, 2\rangle^{(j)}$, only 6 intermediate states are possible:

$$|\Omega\rangle^{(i)} \otimes |2, 1, 0\rangle^{(j)} \quad \text{and} \quad i \leftrightarrow j(S = 0),$$
$$|\Omega\rangle^{(i)} \otimes |2, 0, 2\rangle^{(j)} \quad \text{and} \quad i \leftrightarrow j(S = 2),$$
$$|\Omega\rangle^{(i)} \otimes |2, 0, 4\rangle^{(j)} \quad \text{and} \quad i \leftrightarrow j(S = 4).$$

The corresponding energy shifts are $\epsilon_S = -4t^2/g_S$, or, written in terms of the c_is,

$$\epsilon_0 = -\frac{4t^2}{c_0 + c_2 - 6c_1}, \quad \epsilon_2 = -\frac{4t^2}{c_0 - 3c_1}, \quad \epsilon_4 = -\frac{4t^2}{c_0 + 4c_1}. \tag{6}$$

In this case, the overlap $\langle \nu|H_t|g, S\rangle$ is the same for all virtual tunnelling states $|\nu\rangle$. Therefore, ϵ_S depends only on the difference of scattering lengths a_S. This suggests that control and engineering of the magnetic properties of the system could be achieved using OFR [46, 50]. One can in principle also use magnetic fields to control the scattering properties, but that would inevitably lead to (linear and/or quadratic) Zeeman effects, which would change the structure of $\hat{H}_0$ (equation (3)). Corresponding effects will be discussed elsewhere. The resulting effective spin–spin Hamiltonian in second-order reads

$$\hat{H}_I^{(ij)} = \epsilon_0 \hat{P}_0^{(ij)} + \epsilon_2 \hat{P}_2^{(ij)} + \epsilon_4 \hat{P}_4^{(ij)}. \tag{7}$$

For ^{87}Rb and using the scattering lengths at zero magnetic field, the energy shifts are $\epsilon_0 = -(4t^2/g_0)$, $\epsilon_2 = -0.962(4t^2/g_0)$ and $\epsilon_4 = -0.906(4t^2/g_0)$. Thus, as ϵ_0 is smallest, ^{87}Rb should experience antiferromagnetic behaviour in the GS (cf [24]). For ^{85}Rb, the scattering lengths are negative in the absence of a magnetic field. Thus Hamiltonian (2) is unstable with respect to collapse. One can, however, use OFR (similarly as has been demonstrated using magnetic Feshbach resonances [51]) to achieve $g_S > 0$ for all S. In this case we expect the physics of the ^{85}Rb lattice spinor gas to be similar to the case of ^{87}Rb. Despite the fact that control of magnetic properties is possible using OFR, observation of the GSs requires, in turn, very low temperatures to resolve accurately the different energy shifts.

3.1.2. Lattice Hamiltonian. The Hamiltonian (7) can be easily generalized to the whole lattice, $\hat{H} = \sum_i \hat{H}_{0,i} + \sum_{\langle ij \rangle} \hat{H}_I^{(ij)}$. It can also be transformed into a polynomial of fourth-order in the Heisenberg interaction $\hat{\mathbf{F}}_i \cdot \hat{\mathbf{F}}_j$:

$$\hat{H} = \sum_i \hat{H}_{0,i} + \sum_{\langle ij \rangle} \left[\frac{39\epsilon_0 - 80\epsilon_2}{51} (\hat{\mathbf{F}}_i \cdot \hat{\mathbf{F}}_j) + \frac{9\epsilon_0 - 8\epsilon_2}{102} (\hat{\mathbf{F}}_i \cdot \hat{\mathbf{F}}_j)^2 \right.$$
$$\left. + \left(-\frac{7\epsilon_0}{204} + \frac{10\epsilon_2}{204} + \frac{\epsilon_4}{72} \right) (\hat{\mathbf{F}}_i \cdot \hat{\mathbf{F}}_j)^3 + \frac{7\epsilon_0 + 10\epsilon_4}{1020} (\hat{\mathbf{F}}_i \cdot \hat{\mathbf{F}}_j)^4 \right]. \tag{8}$$

Here all four powers of $\hat{\mathbf{F}}_i \cdot \hat{\mathbf{F}}_j$ appear due to the fact that channels 1 and 3 between different sites are not forbidden.

3.2. Two atoms per site

3.2.1. Accessible single site states. We now derive the effective Hamiltonian for the case in which the GS corresponds to two particles per site and proceed as before by considering the two-site problem. To calculate the energy shifts, we find first the GSs of the unperturbed Hamiltonian $\hat{H}_0$, which are easily determined from equation (4). The GS corresponds to

- $|2, 1, 0\rangle$ if $g_0 < g_2, g_4$, i.e. for $c_1 < 0$, $c_2 < 10c_1$ and $c_1 > 0$, $c_2 < 3c_1$. This singlet state is the single-site GS of ^{87}Rb for unmodified values of scattering lengths.

- $|2, 0, 2\rangle$ if $g_2 < g_0, g_4$, i.e. for $c_1 > 0$, $c_2 > 3c_1$. This situation may be accessed with OFR (see appendix A for details).

- $|2, 0, 4\rangle$ if $g_4 < g_2, g_0$, i.e., for $c_1 < 0$ and $c_2 > 10c_1$; this case is hardly accessible experimentally. Using OFR to achieve it would lead to enormous losses (see appendix A).

In the case of singlets $|2, 1, 0\rangle$, the lattice GS is non-degenerate in zeroth order in t, such that it does not have any effective dynamics. It does, however, have the first order correction to the wave function $|\Psi\rangle = (1 - (\hat{H}_0 - E_0)^{-1}\hat{H}_t) \prod_i |2, 1, 0\rangle$. It has also the second order shift of the GS energy $\delta E = -\langle\psi|\hat{H}_t(\hat{H}_0 - E_0)\hat{H}_t|\psi\rangle$.

3.2.2. Pair Hamiltonian. To calculate the energy shifts to second-order, we assume for simplicity that the energy spacing between eigenstates of $\hat{H}_0$ is sufficiently large compared to tunnelling transitions to intermediate states and treat, therefore, these states as non-degenerate. We shall consider here only the $|2, 0, 2\rangle$ single-site GS, because the state $|2, 0, 4\rangle$ is hardly accessible experimentally. In the latter case, the corresponding effective Hamiltonian admits a very large number of virtual intermediate states and is, therefore, very complex to calculate. We expect, however, that the physics for the cases $|2, 0, 2\rangle$ and $|2, 0, 4\rangle$ is similar.

Starting from $|2, 0, 2\rangle^{(i)} \otimes |2, 0, 2\rangle^{(j)}$, to second order in t there are 26 intermediate virtual states spanning the five channels of total spin $S = 0 - 4$:

$$|1, 0, 2>^{(i)} \otimes|3, 1, 2>^{(j)} \quad \text{and} \quad i \leftrightarrow j(S = 0 \ldots 4),$$
$$|1, 0, 2>^{(i)} \otimes|3, 0, 0>^{(j)} \quad \text{and} \quad i \leftrightarrow j(S = 2),$$
$$|1, 0, 2>^{(i)} \otimes|3, 0, 3>^{(j)} \quad \text{and} \quad i \leftrightarrow j(S = 1 \ldots 4),$$
$$|1, 0, 2>^{(i)} \otimes|3, 0, 4>^{(j)} \quad \text{and} \quad i \leftrightarrow j(S = 2 \ldots 4).$$

The corresponding energy shifts are:

$$\epsilon_0 = -t^2 \frac{(1/7)(124/35)^2}{c_0 + 7/5c_2},$$

$$\epsilon_1 = -t^2 \left[\frac{1}{7}\frac{(22/35)^2}{c_0 + 7/5c_2} + \frac{2}{21}\frac{(144/35)^2}{c_0 + 3c_1}\right],$$

$$\epsilon_2 = -t^2 \left[\frac{1}{7}\frac{(6/7)^2}{c_0 + 7/5c_2} + \frac{1}{15}\frac{(342/49)^2}{c_0 - 3c_1} + \frac{3}{}\frac{(20/49)^2}{c_0 + 3c_1} + \frac{1}{11 \times 35}\frac{(1124/49)^2}{c_0 + 7c_1}\right],$$

$$\epsilon_3 = -t^2 \left[\frac{1}{7}\frac{(8/7)^2}{c_0 + 7/5c_2} + \frac{3}{7}\frac{1}{c_0 + 3c_1} + \frac{9}{11}\frac{21/13}{c_0 + 7c_1}\right],$$

$$\epsilon_4 = -t^2 \left[\frac{1}{7} \frac{(8/7)^2}{c_0 + 7/5c_2} + \frac{(18/7)^2}{c_0 + 3c_1} + \frac{5(11/7)^2}{c_0 + 7c_1} \right].$$

The full effective spin Hamiltonian reads $\hat{H} = \sum_i \hat{H}_{0,i} + \sum_{\langle ij \rangle} (\epsilon_0 \hat{P}_0^{(ij)} + \epsilon_1 \hat{P}_1^{(ij)} + \epsilon_2 \hat{P}_2^{(ij)} + \epsilon_3 \hat{P}_3^{(ij)} + \epsilon_4 \hat{P}_4^{(ij)})$. If scattering lengths are changed through OFR to have $|2, 0, 2\rangle$ as the unperturbed single-site GS, $\hat{H}$ has a ferromagnetic lattice GS $|\Psi\rangle = \bigotimes_i |2, 0, 2\rangle_2^{(i)}$ for ^{87}Rb. The energy shifts of the different spin channels are now mostly determined by the different contributions of the intermediate states $|\nu\rangle$ and Clebsch–Gordon coefficients rather than by the differences in scattering length. As a result we do not expect that OFR will allow precise and extensive control of spin–spin interactions. We expect that in the $|2, 0, 4\rangle$ phase energy shifts exhibit a similar behaviour determined essentially by the values of Clebsch–Gordon coefficients, although the magnetic properties of this phase have yet to be calculated. Quite generally, we conjecture that tuning spin–spin interactions via OFR in systems with two particles per site will be more difficult than for systems with one particle per site.

4. Ground state properties for $F = 2$

In this section we will study the GS properties of systems with one or two particles per site, concentrating on the question of whether the control over the scattering lengths can lead to the appearance of some more exotic phases (cf [52]), assuming a simple 1D chain or a 2D square lattice. To this aim we use the approach developed recently by Wolf *et al* [53], and search for such combinations of parameters for which we can represent the GS of our Hamiltonian exactly (isolated exact GSs), or nearly exactly using MPS [47] in 1D, and PEPS in 2D [54].

First we add to the bond Hamiltonian (7) a certain number of times the identity operator $\hat{I}^{(ij)} = \sum_S \hat{P}_S^{(ij)}$ on the bond, so that the Hamiltonian becomes positive definite, i.e.

$$\hat{H}_I^{(ij)} = \sum_{S=0}^{4} \lambda_S \hat{P}_S^{(ij)}, \tag{9}$$

with all λ_S being non-negative.

In the case of one atom per site (see section 3.1) $\lambda_1 = \lambda_3 > 0$ take the greatest values, whereas one of the λ_S for $S = 0, 2, 4$ can be set to zero. We will subsequently assume that the control over the scattering lengths permits us to choose which one is set to zero and to fix the magnitude of the others, even though this goes beyond experimental feasibility; we will treat experimentally accessible cases with particular attention.

In the case of two atoms per site (see section 3.2), the values of λ_S are essentially determined by the Clebsch–Gordan coefficients. They decrease quite significantly as S increases, with $\lambda_4 = 0$. Thus an extensive control of the effective Hamiltonian using OFR is hardly possible. Nevertheless, in section 4.2 we explore some limiting cases by setting further λ_Ss to zero.

4.1. Searching for isolated exact ground states

Our approach to search for exact (or, at least, 'variationally exact') GSs in 1D with periodic boundary conditions can be described as follows. We seek translationally invariant MPS (see appendix B) of N spins, given by $|\Psi\rangle = \sum_{s_1, s_2, \ldots, s_N} c_{s_1, s_2, \ldots, s_N} |s_1, s_2, \ldots, s_N\rangle$, where s_k

enumerate the computational spin-2 basis. The coefficients $c_{s_1, s_2, \ldots, s_N}$ are parametrized through $d \times d$ matrices A^{s_i}:

$$c_{s_1, s_2, \ldots, s_N} = \sum_{\alpha_1, \alpha_2, \ldots, \alpha_N} A^{s_1}_{\alpha_1, \alpha_2} A^{s_2}_{\alpha_2, \alpha_3} \ldots A^{s_N}_{\alpha_N, \alpha_1}, \tag{10}$$

$$= \mathrm{Tr}(A^{s_1} A^{s_2} \ldots A^{s_N}). \tag{11}$$

Let $R(ij)$ denote the range of the reduced density matrix $\rho_{ij} = \mathrm{Tr}_{k \neq i,j}(|\Psi\rangle\langle\Psi|)$. This range is given by $R(ij) = \mathrm{span}_M \sum_{s_i, s_j} \mathrm{Tr}(M A^{s_i} A^{s_j})|s_i, s_j\rangle$, where the Ms are arbitrary $d \times d$ matrices, whereas $\mathrm{span}_M |\Psi_M\rangle$ denotes the subspace of the Hilbert space spanned by all $|\Psi_M\rangle$s. Let $K(ij)$ denote the kernel of the bond Hamiltonian (9). Note that if $R(ij) \subset K(ij)$, then $\hat{H}|\Psi\rangle = 0$, and since $\hat{H}$ is non-negative, this implies that $|\Psi\rangle$ is a GS. Alternatively, we may search for states that break the translational symmetry; antiferromagnetic Néel-like ordering in 1D could, for instance, correspond to MPS of the form $|\Psi\rangle = \sum_{s_1, s_2, \ldots, s_N} \mathrm{Tr}(A^{s_1} B^{s_2} A^{s_3} \ldots B^{s_N})|s_1, s_2, \ldots, s_N\rangle$ for even N. A similar procedure can be applied in 2D using PEPS, a generalization of MPS.

4.2. One atom per site

4.2.1. Mean field diagram. Before we proceed, it is worth discussing the mean field phase diagram obtained under the assumption that the GS is a product state, $|\Psi\rangle = |e, e, \ldots\rangle$ (see [24, 28]). We are following here the most complete description of the phase diagram, provided recently in [28]. We introduce the nematic tensor $Q_{ab} = \frac{1}{2}\langle \hat{F}_a \hat{F}_b + \hat{F}_b \hat{F}_a \rangle - \frac{1}{3}\delta_{ab}\langle \hat{\mathbf{F}}^2 \rangle$. There are three possible mean field (i.e. product) GSs, with $|e\rangle$ given, up to $SO(3)$ rotations.

1. Ferromagnetic state, $|e\rangle = (1, 0, 0, 0, 0)$; possesses only the $U(1)$ symmetry of rotations around the z-axis, and has maximal projection of the spin onto z-axis.
2. Nematic state, $|e\rangle = (\sin(\eta)/\sqrt{2}, 0, \cos(\eta), 0, \sin(\eta)/\sqrt{2})$; apart from $SO(3)$ rotation has an additional η-degeneracy. This state is a MI version of the polar state in BEC. It has mean value of all components of the spin equal zero, but non vanishing singlet projection $\langle \mathrm{singlet}|e, e\rangle \neq 0$.
3. Tetrahedratic (cyclic) state, $|e\rangle = (1/\sqrt{3}, 0, 0, \sqrt{2/3}, 0)$; this is a MI version of the cyclic state. The state may be uni- or biaxial, depending on whether the nematic tensor does, or does not have a pair of degenerated eigenvalues; it has vanishing of both the mean values of all of the spin components, and of the singlet projection.

The phase diagram is such that the system is in

1. a ferromagnetic state for $\lambda_4 = 0$, $\lambda_2, \lambda_0 > 0$, and for $\lambda_0 = 0$, provided $\lambda_2 \geqslant 17\lambda_4/10$;
2. a nematic state for $\lambda_0 = 0$, provided $3\lambda_4/10\lambda_2 \leqslant 17\lambda_4/10$;
3. a cyclic state for $\lambda_0 = 0$, provided $\lambda_2 \leqslant 3\lambda_4/10$, and for $\lambda_2 = 0$.

We will identify below the regimes of the phase diagram in which the mean field diagram is exact, or nearly exact.

4.2.2. MPS reduce to mean field states. Since $\lambda_1 = \lambda_3 > 0$ take the greatest values, the GS of (9) should belong to the symmetric subspace. For translationally invariant MPS this implies $[A^{s_i}, A^{s_j}] = 0, \forall s_i, s_j$. Then the same matrix K transforms A^i and A^j into the commuting Jordan forms. Generically, if all eigenvalues $\lambda_\alpha^{s_i}$ of A^{s_i} are distinct for each s_i, then the matrices A can be diagonalized, and

$$|\psi\rangle = \sum_{s_1,...s_N} \sum_\alpha \lambda_\alpha^{s_1} \ldots \lambda_\alpha^{s_N} |s_1, \ldots s_N\rangle \equiv \sum_\alpha h_\alpha^N |e_\alpha, \ldots, e_\alpha\rangle, \qquad (12)$$

where $|e_\alpha\rangle = h_\alpha^{-1} \sum_s \lambda_\alpha^s |s\rangle$, and h_α are chosen in order to normalize states $|e_\alpha\rangle$ correctly. Since the Hamiltonian is a sum of nearest neighbour bond Hamiltonians, we have $\langle e_\alpha, e_\alpha \ldots | \hat{H}_I | e_{\alpha'}, e_{\alpha'} \ldots \rangle \propto \langle e_\alpha | e_{\alpha'} \rangle^{N-2}$ in a 1D chain, and thus in the limit of an infinite chain the GSs are equally well described by product states $|e_\alpha, \ldots, e_\alpha\rangle$ that will typically break the rotational symmetry. Because of the same symmetry, they will enter the sum over α in equation (12) with equal weights $|h_\alpha|^N = |h|^N$, and be quasi-degenerated in the large N limit. This means in this case we expect mean field (product) states to provide a very good approximation of the GSs with translational symmetry.

4.2.3. Possible configurations of the λs. We will now identify exact or variational GSs for various combinations of the λs.

(A₁) For $\lambda_4 = \lambda_2 = \lambda_0 = 0$, all symmetric states are GSs, i.e. in particular all product states $|e, e \ldots\rangle$ with arbitrary $|e\rangle$.

(B₁) For $\lambda_4 = \lambda_2 = 0$, $\lambda_0 > 0$, the GSs $|e, e \ldots\rangle$ resemble the cyclic states of [15] (i.e. they correspond to translationally but not rotationally invariant product states), which now mix $S = 2$ and 4 contributions on each bond, and they have to fulfil the condition $\langle \text{singlet} | e, e \rangle = 0$. Denoting $|e\rangle = (e_2, e_1, e_0, e_{-1}, e_{-2})$, this implies $e_0^2 - 2e_1 e_{-1} + 2e_2 e_{-2} = 0$. These states form a much greater class than the cyclic ones, since they may have non-vanishing (and even maximal) components of the spin. Interestingly, the transition between the cyclic phase for $\lambda_2 = 0$, and the ferromagnetic phase for $\lambda_4 = 0$, occurs via such states, i.e. at the transition point the degeneracy of the GSs manifold explodes.

(C₁) For $\lambda_4 = 0$ and $\lambda_2, \lambda_0 > 0$, the GSs are ferromagnetic states $|2\rangle_\mathbf{n} |2\rangle_\mathbf{n} \ldots |2\rangle_\mathbf{n}$, corresponding to a maximal projection of the local spin on to a given direction $\mathbf{n} = (\sin(\theta)\cos(\phi), \sin(\theta)\sin(\phi), \cos(\theta))$. Such vectors for $F = 2$ may be parametrized (in the basis of $\hat{\mathbf{F}}_\mathbf{n}$ with descending m_F) as $\propto (z^{-2}, 2z^{-1}, \sqrt{6}, 2z, z^2)$ with $z = |z| e^{i\phi}$, $|z| \in (-\infty, \infty)$. It should be stressed that ferromagnetic states are *exact* GS in the entire part of the phase diagram whenever $\lambda_4 = 0$.

(D₁) For $\lambda_0 = 0$ and $\lambda_4, \lambda_2 > 0$, the GSs apparently favour antiferromagnetic order. This, however, can be misleading, if $\lambda_4 \ll \lambda_2$. In that case, as the mean field diagram suggests, the ferromagnetic order might prevail. We have applied in 1D a more general variational approach, going beyond mean field. We have looked for GSs by applying the variational principle to mean field (product) states $|e, e \ldots\rangle$, Néel-type states $|e, f, e, f \ldots\rangle$, and valence bond solid states with singlet states for distinct pairs (dimers) of neighbouring atoms and translational dimer symmetry. For the mean field case as discussed earlier the energy is either minimized by the ferromagnetic state $|e\rangle = |2\rangle_\mathbf{n}$ (for $\lambda_2 \geqslant 17\lambda_4/10$), by a nematic state $|e\rangle = |0\rangle_\mathbf{n}$ (for $3\lambda_4/10 \leqslant \lambda_2 \leqslant 17\lambda_4/10$; in this case the state is a combination of total spin 0, 2 and 4), or, for $\lambda_2 \leqslant 3\lambda_4/10$, by a cyclic
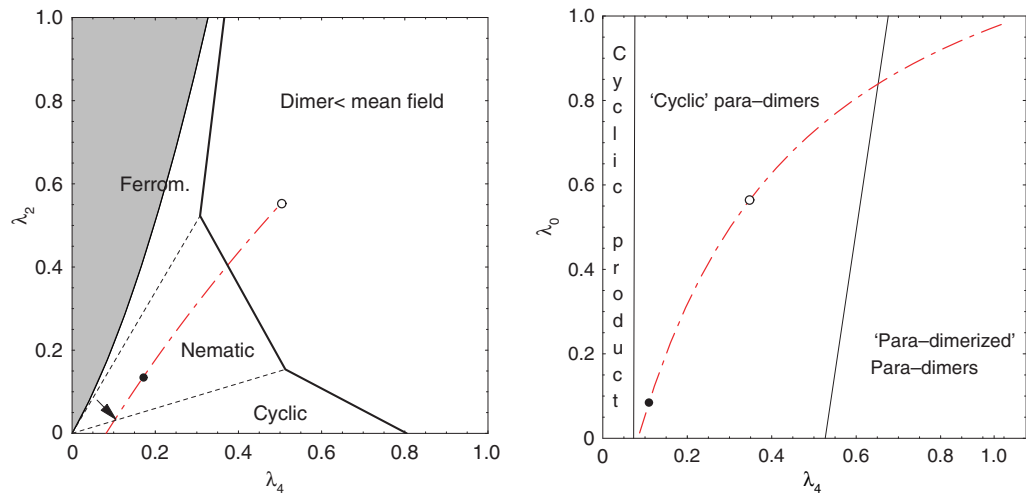
Figure 1. (a) Sketch of the phase diagram for the (D_1) case, obtained by applying the variational principle in the λ_2, λ_4 phase space (for $\lambda_0 = 0$) to mean field, Néel, and dimer states with one atom per site. The scale is set by letting $\lambda_1 = \lambda_3 = 1$. Néel-type states are never favourable over nematic states. The *ferromagnetic* region (grey) was obtained numerically by imaginary time evolution of MPS, and comparing the result from runs with $d = 1$ and 5 in a chain of 50 sites with open boundary conditions [55]. Of course, on the line $(\lambda_4 = 0, \lambda_2)$ ferromagnetic states always give GS. Dashed lines indicate the regions where the type of mean field state with lowest energy changes qualitatively (see text for more details). The red (dashed-dotted) line gives the values of (λ_2, λ_4) which can be obtained by changing the spin-independent scattering length $\bar{c}_0 = (3\bar{g}_4 + 4\bar{g}_2)/7$ of ^{87}Rb through OFR. The arrow gives the values for unchanged $\bar{c}_0$, black and white circles indicate a change of $\bar{c}_0$ of 10 and 100%, respectively. (b) Sketch of the phase diagram for the case (E_1), i.e. when λ_2 is the lowest coefficient. The Hamiltonian is shifted and rescaled such that $\lambda_2 = 0, 0 \leqslant \lambda_0, \lambda_4 \leqslant 1$, and $\lambda_1 = \lambda_3 = 1$. The lines give the boundaries obtained from variationally comparing product states (where cyclic states are always optimal) to product states of para-dimers (where again the cyclic combination gives minimal energy), and to combinations of neighbouring para-dimers with total spin $S' = 2$. The red (dotted–dashed) line indicates the combinations of (λ_4, λ_0) which can be obtained by changing $\bar{c}_0$ through an OFR. Black and white circles indicate a change of $\bar{c}_0$ of -10 and -50%, respectively.

state, $|e\rangle = (e_2, e_1, e_0, e_{-1}, e_{-2})$ with $e_0 = 1/\sqrt{2}$, $e_2 = -e_{-2} = 1/2$, $e_1 = e_{-1} = 0$. Imposing Néel order with $\langle e|f\rangle \neq 1$ always results in a larger energy, as $\lambda_{1,3} > \lambda_{2,4}$, and the overlap with the singlet can be maximized already by restricting to product states. On the other hand, for the dimer state the energy per bond is given by $\frac{1}{2}\text{Tr}(H_I \frac{1}{25} \mathbb{1} \otimes \mathbb{1})$. This results in the phase diagram shown in figure 1, somewhat analogous to the results obtained by Yip [16]. The red line depicts values of λ_2, λ_4 experimentally accessible through modifications of scattering lengths. We have applied MPS code to search numerically for the exact GSs using the method of [55]. We confirmed that in the shaded region in figure 1 (a) there is indeed a ferromagnetic GS. We have also studied the GS at the experimentally accessible line, and found indications of nematic
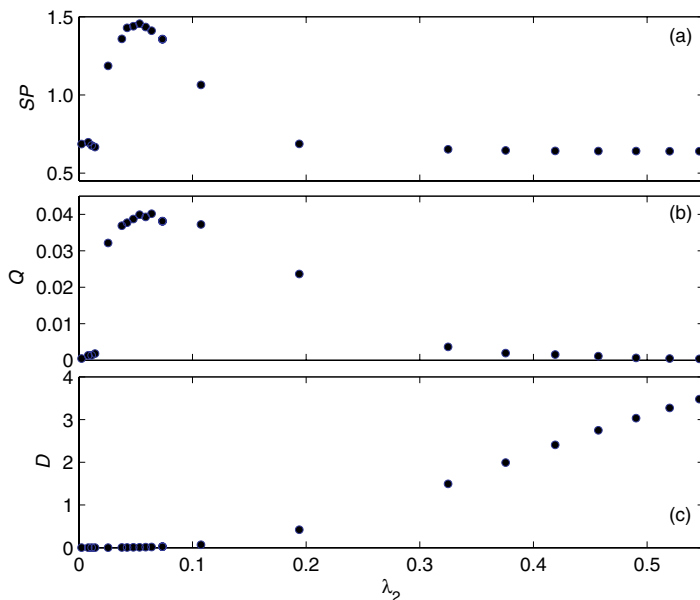
Figure 2. Analysis of the GSs obtained variationally from an MPS ansatz for the case (D$_1$), for combinations of λ_2 and λ_4 lying on the dotted-dashed line of figure 1. (a) Singlet projection $SP = \sum_i \text{tr}(\hat{P}_0 \rho_i \otimes \rho_i)$, where ρ_i is the reduced density matrix of site i, (b) nematic order parameter $Q = \max_\omega Q_\Omega = \max_\Omega \sum_i [(\vec{n}_\Omega \vec{S}_i)^2 - 2]/N$ ($\vec{n}_\Omega$ is the unit vector pointing in direction Ω), and (c) dimerization $D = |\langle \hat{P}_0^{N/2,N/2+1}\rangle - \langle \hat{P}_0^{N/2-1,N/2}\rangle|$ (values obtained for open chains of 16 sites, with $d = 30$).

and dimer order in the phase diagram, see figure 2. We expect that in 2D, in addition a possible GS could be formed from resonating valence bond states [52], and we are planning to apply the 2D PEPS methods to investigate this question.

(E$_1$) For $\lambda_2 = 0$ and λ_4, $\lambda_0 > 0$, as in the (D$_1$) case, mean field cyclic states are favourable over Neél states. We have compared them variationally to the analogues of the dimer states in the present case, i.e. configurations which have a state with total spin $S = 2$ on distinct bonds. We call these state *para-dimers*. Now the situation is quite different from the dimerized states discussed in (D$_1$), as the states on the bond are not unique and states with different total spin projection $M_{S=2}$ can form superpositions. In the subspace of states having a para-dimer on each second bond, the Hamiltonian can be written as an effective interaction between neighbouring para-dimers, $(H'_{\text{eff}})_{(ij)} = \sum_{S'=0}^4 \lambda_{S'} (P')_{S'}^{(ij)}$, where i, j now enumerate the para-dimers, and $(P')_{S'}$ projects on to the subspace of two para-dimers with total spin S'. For $\lambda_2 = 0$, λ_0, $\lambda_4 > 0$, always $\lambda'_2 < \lambda'_0, \lambda'_4$, and the optimal superposition of para-dimers with different projections is again the cyclic combination. On the other hand, given that λ'_2 is the lowest coefficient, combining neighbouring para-dimers to states with total spin $S' = 2$ might lead to even lower energies. On this level again states with different total z-projection $M_{S'}$ can be combined, and it turns out that again the cyclic combination minimizes the energy. Comparing the energies of cyclic product states, cyclic states of para-dimers, and cyclic combinations of 'para-dimerized' para-dimers, the phase diagram shown in figure 1(b) is obtained.

4.3. Two atoms per site

We discuss here cases where the values of the λ_S are in descending order, determined essentially by the Clebsch–Gordan coefficients. In such a situation only a ferromagnetic-like order in the GS is possible, but now the states do not necessarily have to be of the product form, especially if $\lambda_1 = 0$, or $\lambda_1 = \lambda_3 = 0$. We explore the following limiting cases.

(A_2) For all $\lambda_S = 0$ except $\lambda_0 > 0$, the GS, when reduced to neighbouring sites, are either of the type $|2\rangle_{\mathbf{n}}|e\rangle$ (or $|e\rangle|2\rangle_{\mathbf{n}}$) with $|e\rangle = (e_2, e_1, e_0, e_{-1}, 0)$ in the $\mathbf{S}_n$ basis; or of the form $|1\rangle_{\mathbf{n}}|\tilde{e}\rangle$ with $|\tilde{e}\rangle = (e_2, e_1, e_0, 0, 0)$ (or $|\tilde{e}\rangle|1\rangle_{\mathbf{n}}$).

(B_2) Similarly, for $\lambda_2 = \lambda_3 = \lambda_4 = 0$ and $\lambda_0, \lambda_1 > 0$, GS correspond to product states which, when reduced to neighbouring sites, have either the form $|2\rangle_{\mathbf{n}}|e\rangle$ (or $|e\rangle|2\rangle_{\mathbf{n}}$) with $|e\rangle = (e_2, e_1, e_0, 0, 0)$ written in the $\mathbf{S}_{\mathbf{n}}$ basis, or the form $|1\rangle_{\mathbf{n}}|1\rangle_{\mathbf{n}}$.

(C_2) For $\lambda_3 = \lambda_4 = 0$ and all other $\lambda_S > 0$, the GSs are product states formed by the vectors $|2\rangle_{\mathbf{n}}$, and $|1\rangle_{\mathbf{n}}$, with the constraint that there are not two $|1\rangle_{\mathbf{n}}$ states in the neighbouring sites.

(D_2) for $\lambda_4 = 0$ and all other $\lambda_S > 0$, the GSs are as in the case (C_1) before, i.e. they are of the form $|2\rangle_{\mathbf{n}}|2\rangle_{\mathbf{n}} \ldots |2\rangle_{\mathbf{n}}$.

5. $F = 3/2$ Fermi–Hubbard Hamiltonian

5.1. The system

Let us now turn to the discussion of the spin-3/2 (in this and the next section) and -5/2 (in sections 7 and 8) Fermi lattice gases. The total wavefunction of the fermions has to be anti-symmetric, implying that the spin of two colliding fermions can only be even. Interaction for two fermions with spin F in the s-wave channel can be written in the form

$$\hat{V} = \bar{g}_0 \hat{P}_0 + \bar{g}_2 \hat{P}_2 + \ldots + \bar{g}_{2F-1} \hat{P}_{2F-1}, \tag{13}$$

where $\hat{P}_S$ is the projection operator on the subspace with total spin S and $\bar{g}_S$ is the interaction strength, which depends on the scattering length (a_S) through $\bar{g}_S = 4\pi\hbar^2 a_S/m$.

5.2. On-site Hamiltonian

For two spin-3/2 particles with anti-symmetric spin-wavefunction, we can use the identities $\hat{I} = \hat{P}_0 + \hat{P}_2$ and $\hat{\mathbf{F}}_1 \ldots \hat{\mathbf{F}}_2 = \gamma_0 \hat{P}_0 + \gamma_2 \hat{P}_2$ to express the interaction in the form ($\hat{V} = \bar{c}_0 \hat{1} + \bar{c}_2 \hat{\mathbf{F}}_1 \cdots \hat{\mathbf{F}}_2$. Here, $\hat{\mathbf{F}}_i$ is the spin operator of the particle i and $\gamma_S = [S(S+1) - 2F(F+1)]/2$. The total Hamiltonian in the limit of vanishing tunnelling ($t = 0$) for $F = 3/2$ is a sum of single-site Hamiltonians of the form (omitting site indices)

$$\hat{H}_0 = \frac{c_0}{2} \sum_{\alpha\beta} \hat{a}^\dagger_\alpha \hat{a}^\dagger_\beta \hat{a}_\beta \hat{a}_\alpha + \frac{c_2}{2} \sum_{\alpha\beta\gamma\sigma} \hat{a}^\dagger_\alpha \hat{a}^\dagger_\beta (F_{3/2})_{\alpha\gamma} (F_{3/2})_{\beta\sigma} \hat{a}_\sigma \hat{a}_\gamma, \tag{14}$$

where $c_0 = (-g_0 + 5g_2)/4$ and $c_2 = (-g_0 + g_2)/3$, and symbols without bars are related to those with bars in the same way as in the bosonic sections. In the summation, greek letters are spin indices. The eigenvalues of the Hamiltonian $\hat{H}_0$ read

$$E^0(N, \bar{F}) = \tfrac{1}{2}c_0 N(N-1) + \tfrac{1}{2}c_2 \left[\bar{F}(\bar{F}+1) - \tfrac{15}{4}N\right], \tag{15}$$
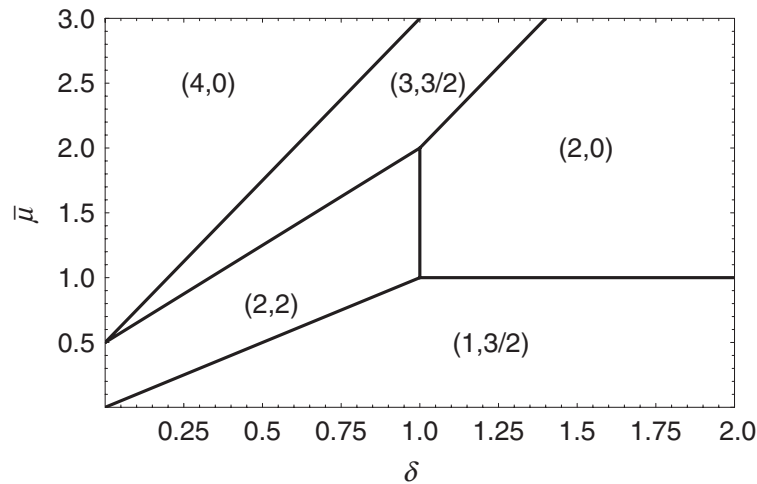
Figure 3. GSs for $F = 3/2$ for the case of no tunnelling, in the space of $\delta = g_2/g_0$ and $\bar{\mu} = \mu/g_0$. The phases are labelled by $(N, \bar{F})$, where N denotes the number of particles per site and $\bar{F}$ their total spin.

where N is the number of particles per site and $\bar{F}$ is the total on-site spin. As there are four accessible states per site, corresponding to the spin projections, the maximal number of particles is $N = 4$.

5.2.1. Phases at $t = 0$. The actual GS in the case of vanishing tunnelling is determined by comparing the (Gibbs potential) energies $G = E_0(N, \bar{F}) - \mu N$ of the above listed states. The resulting phase diagram is already quite complex and depends on the values of c_0 and c_2, or better to say g_0, g_2, in a nontrivial way (see figure 3). Denoting the states by $(N, \bar{F})$, and writing $\delta = g_2/g_0$ and $\bar{\mu} = \mu/g_0$, we obtain

1. $(0,0)$ is the GS for $\bar{\mu} < 0$;
2. $(1,3/2)$ is the GS for $0 < \bar{\mu} < 1$, and $\bar{\mu} < \delta$;
3. $(2,0)$ is the GS for $1 < \bar{\mu} < (5\delta - 1)/2$, and $\delta > 1$;
4. $(2,2)$ is the GS for $\delta < 1$, and $\delta < \bar{\mu} < (3\delta + 1)/2$;
5. $(3,3/2)$ is the GS for $\max[(3\delta + 1)/2, (5\delta - 1)/2] < \bar{\mu} < (5\delta + 1)/2$;
6. $(4,0)$ is the GS for $(5\delta + 1)/2 < \bar{\mu}$.

6. Effective Hamiltonian for $F = 3/2$

We follow here the same line as in the bosonic part to derive an effective spin–spin Hamiltonian, applying equation (5) to calculate energy shifts to second order in t.

Very recently, Tu *et al* [56] have studied spin quadrupole ordering in spin-$3/2$ gases and derived effective spin Hamiltonians for the first and second MI lobe. Our results agree with theirs and provide a complementary approach and discussion.

6.1. One atom per site

For a single particle per site and $t = 0$, the two-site state with total spin S and maximal total z-projection reads

$$|SM_S = S\rangle_{i,j} = \sum_{m_1, m_2} \langle FFm_1m_2|SM_S = S\rangle a^\dagger_{im_1} a^\dagger_{jm_2}|\Omega\rangle, \tag{16}$$

where F is a spin of a fermion (m_1, m_2 are the z-components of this spin), and i and j are lattice indices. Possible intermediate states are those having two particles on one site (say i), and no particles on the other (say j). Two-particle states with total on-site spin $\bar{F}$ and maximal projection $M_{\bar{F}} = \bar{F}$ read

$$|\nu\rangle_{ij} = |\bar{F}, M_{\bar{F}} = \bar{F}\rangle_{ij} = \frac{1}{\sqrt{2}} \sum_{m_1 \neq m_2} \langle FFm_1m_2|\bar{F}, m_{\bar{F}} = \bar{F}\rangle a^\dagger_{im_1} a^\dagger_{im_2}|\Omega\rangle. \tag{17}$$

From anti-commutation relations for fermions and properties of Clebsch–Gordon coefficients, it follows that $\bar{F}$ has to be even. The energy shifts thus are simply $\epsilon_S = -\frac{4t^2}{g_S}$ for even total spin S, and $\epsilon_S = 0$ otherwise. The explicit expressions for $F = 3/2$ can be written

$$\epsilon_2 = -\frac{4t^2}{g_2} = -\frac{4t^2}{c_0 - 3c_2/4}, \qquad \epsilon_0 = -\frac{4t^2}{g_0} = -\frac{4t^2}{c_0 - 15c_2/4} \tag{18}$$

(and $\epsilon_3 = \epsilon_1 = 0$) and the effective Hamiltonian is $\hat{H}_1^{(ij)} = \epsilon_0 \hat{P}_0^{(ij)} + \epsilon_2 \hat{P}_2^{(ij)}$. This result is the same as discussed in [56, 57]. The effective spin model has several particularly interesting limits. In particular, when $g_0 = g_2$ the model has a $SU(4)$ symmetry, and is integrable via the Bethe ansatz in 1D [58]; its GS is a spin singlet with gapless excitations.

6.2. Two atoms per site

For two spin-3/2 fermions on each lattice site the total on-site spin $\bar{F}$ may take values 0 or 2. We express two-site states with total spin S in the form $|S, \bar{F}\rangle$ (again we limit to the maximal total z-component $M_S = S$). We write the states in the same form as in equation (16)

$$|S, \bar{F}\rangle_{i,j} = \frac{1}{2} \sum_{m_1, m_2, n_1, n_2, \bar{M}, \bar{N}} \langle \bar{F}\bar{F}\bar{M}\bar{N}|SM_S = S\rangle \langle FFm_1m_2|\bar{F}\bar{M}\rangle \langle FFn_1n_2|\bar{F}\bar{N}\rangle a^\dagger_{im_1} a^\dagger_{im_2} a^\dagger_{jn_1} a^\dagger_{jn_2}|\Omega\rangle, \tag{19}$$

where $\bar{M}, \bar{N}$ are the z-components of the total spins of sites i, j, respectively. If the on-site states are singlets, i.e. $\bar{F} = 0$, there is no effective interaction to second-order in t, but there is a second-order shift which amounts to $\epsilon_0 = -2t^2/(c_0 + 15c_2/4)$ per bond. For $\bar{F} = 2$, constructing the intermediate states with three fermions in site i and one in site j, the energy shifts can be calculated as $\epsilon_4 = \epsilon_2 = 0$ and

$$\epsilon_3 = \epsilon_1 = -\frac{4t^2}{c_0 - 9c_2/4}, \quad \epsilon_0 = -\frac{10t^2}{c_0 - 9c_2/4}. \tag{20}$$

The above results agree with those obtained recently in [56].

6.3. Three atoms per site

For three particles per lattice site, possible two-site states are similar to the case of one atom per site, equation (17), because states of three atoms per site can equivalently be written as a single hole in the filled Fermi sea. Intermediate states now have four particles on one site. Because of Pauli's principle there is only one such state, namely the filled Fermi sea $a^\dagger_{i,3/2} a^\dagger_{i,1/2} a^\dagger_{i,-1/2} a^\dagger_{i,-3/2} |\Omega\rangle$. It is thus clear that the energy shifts have to be as in equation (18).

Obviously, for four particles per site the on-site GS is the filled Fermi sea. This is an exact eigenstate of the full Hamiltonian, as no tunnelling is possible in this state.

7. $F = 5/2$ Fermi–Hubbard Hamiltonian

The theory for insulating states of a spin-5/2 gas with 1 or 2 atoms per lattice site is essentially the same as in the case of spin-3/2 particles, so we will comment only the basic differences.

7.1. The system and on-site states

Now the two-particle s-wave interaction can be written in the form

$$\hat{V} = \bar{g}_0 \hat{P}_0 + \bar{g}_2 \hat{P}_2 + \bar{g}_4 \hat{P}_4 \tag{21}$$

or, using the identity operator $\hat{I}$ and spin operators $\hat{\mathbf{F}}_i$,

$$\hat{V} = \bar{c}_0 \hat{1} + \bar{c}_1 (\hat{\mathbf{F}}_i \ldots \hat{\mathbf{F}}_j) + \bar{c}_2 \hat{P}_0, \tag{22}$$

where $\bar{c}_0 = (5\bar{g}_2 + 23\bar{g}_4)/28$, $\bar{c}_1 = (-\bar{g}_2 + \bar{g}_4)/7$, and $\bar{c}_2 = (7\bar{g}_0 - 10\bar{g}_2 + 3\bar{g}_4)/7$. The singlet projection operator $\hat{P}_0$ can be represented via creation and annihilation operators as

$$\hat{P}_0 = \hat{A}^\dagger \hat{A}, \tag{23}$$

$$\hat{A} = -\frac{1}{\sqrt{3}} \left(\hat{a}_{5/2} \hat{a}_{-5/2} - \hat{a}_{3/2} \hat{a}_{-3/2} + \hat{a}_{1/2} \hat{a}_{-1/2} \right). \tag{24}$$

The on-site Hamiltonian attains then a similar form as in the case of spin-3/2 with an additional term $c_2 \hat{P}_0$ (and relations between $\bar{c}_i$ and c_i as before). The energies for different numbers of fermions per site N and total on-site spin $\bar{F}$ are listed below:

$$E^0(N = 1, \bar{F} = 5/2) = 0, \tag{25a}$$

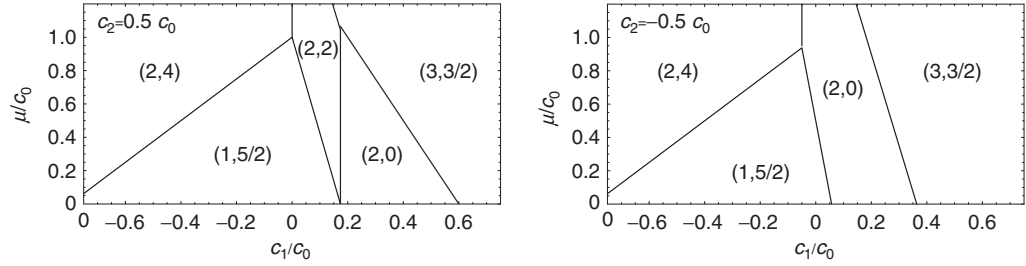$$E^0(N = 2, \bar{F} = 4) = c_0 + \tfrac{5}{4} c_1, \tag{25b}$$

$$E^0(N = 2, \bar{F} = 2) = c_0 - \tfrac{23}{4} c_1, \tag{25c}$$

$$E^0(N = 2, \bar{F} = 0) = c_0 - \tfrac{35}{4} c_1 + c_2, \tag{25d}$$

$$E^0(N = 3, \bar{F} = 9/2) = 3c_0 - \tfrac{3}{4} c_1, \tag{25e}$$

$$E^0(N = 3, \bar{F} = 5/2) = 3c_0 - \tfrac{35}{4} c_1 + \tfrac{2}{3} c_2, \tag{25f}$$

$$E^0(N = 3, \bar{F} = 3/2) = 3c_0 - \tfrac{45}{4} c_1. \tag{25g}$$

Figure 4. GS for $F = 5/2$ for the case of no tunnelling, in the space of c_1/c_0 and $\bar{\mu} = \mu/g_0$ for $c_2/c_0 = 1/2$ (left) and $c_2/c_0 = -1/2$ (right), taking into account states of up to three particles. The phases are labelled by $(N, \bar{F})$, where N denotes the number of particles per site and $\bar{F}$ their total spin.

7.2. Phase at $t = 0$

The actual GS are determined by minimizing the Gibbs energy $G = E_0(N, \bar{F}) - \mu N$. The resulting phase diagram is 3D and quite complex, as it depends on the values of c_0, c_1 and c_2 (or better to say g_0, g_1 and g_2) in a highly nontrivial way. The GS are plotted in the space of μ/c_0 and c_1/c_0 for two values of c_2 in figure 4.

8. Effective Hamiltonian for $F = 5/2$

8.1. One atom per site

The effective Hamiltonian to second-order in the tunnelling amplitude t has the form $\hat{H}_{\mathrm{I}}^{(ij)} = \epsilon_0 \hat{P}_0^{(ij)} + \epsilon_2 \hat{P}_2^{(ij)} + \epsilon_4 \hat{P}_4^{(ij)}$, where

$$\epsilon_4 = -\frac{4t^2}{g_4} = -\frac{4t^2}{c_0 + \frac{5}{4}c_1}, \qquad \epsilon_2 = -\frac{4t^2}{g_2} = -\frac{4t^2}{c_0 - \frac{23}{4}c_1}, \tag{26a}$$

$$\epsilon_0 = -\frac{4t^2}{g_0} = -\frac{4t^2}{c_0 - \frac{35}{4}c_1 + c_2}. \tag{26b}$$

As usually ϵ_4 is smallest, the GS in this case are mostly ferromagnetic, as can be seen from figure 5(a). There is however a region where $\epsilon_0 < \epsilon_2, \epsilon_4$. In this case the variational approach followed in section 4, case (D_1) shows that within this region again dimerized as well as ferromagnetic, nematic, or cyclic phases might be realized (see figure 5(b)).

8.2. Two atoms per site

On-site GS with two fermions per site can have total spin 0, 2, or 4. Tunnelling carries over these states into those with three atoms on one site, and one on the neighbouring site. The state of three particles on lattice site i with total spin $\bar{F}$ and z-projection $\bar{M}$ can be written in the form

$$|\bar{F}\bar{M}\rangle \propto \sum_{m_1,m_2,m_3,\bar{F}_2,\bar{M}_2} \langle F F m_1 m_2 | \bar{F}_2 \bar{M}_2 \rangle \langle \bar{F}_2 F \bar{M}_2 m_2 | \bar{F}\bar{M} \rangle a^{\dagger}_{i,m_1} a^{\dagger}_{i,m_2} a^{\dagger}_{i,m_3} |\Omega\rangle. \tag{27}$$
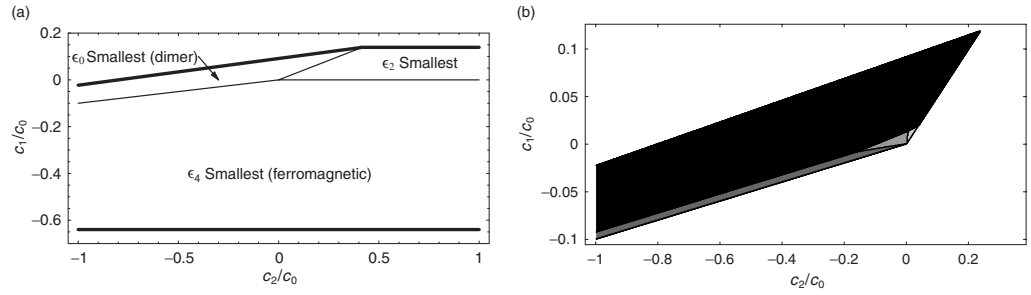
Figure 5. (a) Classification of the effective Hamiltonians which can be obtained for $F = 5/2$ and a single particle per site (see equation (26)) in the $(c_1/c_0, c_2/c_0)$ space (for $\mu/c_0 = 0.2$). Thick lines indicate the borders of the region where the $t = 0$ GS has a single particle per site, thin lines indicate the borders between different regimes of the corresponding effective Hamiltonian. When ϵ_4 is lowest, then the GS is ferromagnetic. The area with $\epsilon_0 < \epsilon_2, \epsilon_4$, is shown in more detail in (b). The different regions are obtained from a variational ansatz similar to section 4, case (D$_1$), comparing dimer with different mean field type states. Lowest energy states according to this ansatz are mostly dimerized (black). The ferromagnetic (dark grey), nematic (grey), and cyclic (light grey) regions are much smaller.

As the virtual state necessarily has to be anti-symmetric, there are three different possibilities for $\bar{F}$, namely 9/2, 5/2, or 3/2. Let us now consider GSs with different on-site spin $\bar{F}$ separately. The case $\bar{F} = 0$ leads only to a GS energy shift, but not to interesting dynamics in second-order perturbation theory.

8.2.1. On-site GS with spin 4. In this case nearest–neighbour pairs can form total spin from $S = 0$ to $S = 8$. The effective Hamiltonian in second-order perturbation theory can be written in the form $H_{\mathrm{I}}^{(ij)} = \sum_S \epsilon_S \hat{P}_S^{(ij)}$, with

$$\epsilon_8 = 0, \tag{28a}$$

$$\epsilon_7 = -\frac{4t^2}{c_0 - (13/4)c_1}, \tag{28b}$$

$$\epsilon_6 = 0, \tag{28c}$$

$$\epsilon_5 = -\frac{(15/7)t^2}{c_0 - (13/4)c_1} - \frac{(13/7)t^2}{c_0 - (45/4)c_1 + (2/3)c_2}, \tag{28d}$$

$$\epsilon_4 = -\frac{(7865/2058)t^2}{c_0 - (13/4)c_1} - \frac{(143/98)t^2}{c_0 - (45/4}c_1 + (2/3)c_2} - \frac{(572/1029)t^2}{c_0 - (55/4)c_1}, \tag{28e}$$

$$\epsilon_3 = -\frac{(1875/686)t^2}{c_0 - (13/4)c_1} - \frac{(11/98)t^2}{c_0 - (45/4)c_1 + (2/3)c_2} - \frac{(396/343)t^2}{c_0 - (55/4)c_1}, \tag{28f}$$

$$\epsilon_2 = -\frac{(297/343)t^2}{c_0 - (13/4)c_1} - \frac{(33/49)t^2}{c_0 - (45/4)c_1 + (2/3)c_2} - \frac{(396/343)^2}{c_0 - (55/4)c_1}, \tag{28g}$$

$$\epsilon_1 = -\frac{(24/7)t^2}{c_0 - (45/4)c_1 + (2/3)c_2} - \frac{(4/7)t^2}{c_0 - (55/4)c_1}, \tag{28h}$$

$$\epsilon_0 = -\frac{6t^2}{c_0 - (45/4)c_1 + (2/3)c_2}. \tag{28i}$$

Tuning c_1/c_0 and c_2/c_0, typically either ϵ_8 and ϵ_6, ϵ_7, or ϵ_4 are the smallest coefficients, such that, though often ferromagnetic GSs are realized, also models preferring antiferromagnetic order are possible.

8.2.2. On-site GSs with spin 2. Finally, we consider the case of on-site GSs with spin 2, where

$$\epsilon_4 = -\frac{(825/686)t^2}{c_0 + (43/4)c_1} - \frac{(45/98)t^2}{c_0 + (11/4)c_1 + (2/3)c_2} - \frac{(60/343)t^2}{c_0 + (1/4)c_1}, \tag{29a}$$

$$\epsilon_3 = -\frac{(825/686)t^2}{c_0 + (43/4)c_1} - \frac{(81/98)t^2}{c_0 + (11/4)c_1 + (2/3)c_2} - \frac{(676/343)t^2}{c_0 + (1/4)c_1}, \tag{29b}$$

$$\epsilon_2 = -\frac{(150/343)t^2}{c_0 + (43/4)c_1} - \frac{(50/147)t^2}{c_0 + (11/4)c_1 + (2/3)c_2} - \frac{(200/343)t^2}{c_0 + (1/4)c_1}, \tag{29c}$$

$$\epsilon_1 = -\frac{(4/7)t^2}{c_0 + (11/4)c_1 + (2/3)c_2} - \frac{(24/7)t^2}{c_0 + (1/4)c_1}, \tag{29d}$$

$$\epsilon_0 = -\frac{(10/3)t^2}{c_0 + (11/4)c_1 + (2/3)c_2}. \tag{29e}$$

Now the effective Hamiltonian is $H_{\text{eff}} = \sum_i H_{0,i} + \sum_{\langle ij \rangle} \epsilon_0 \hat{P}_0^{ij} + \epsilon_1 \hat{P}_1^{ij} + \epsilon_2 \hat{P}_2^{ij} + \epsilon_3 \hat{P}_3^{ij} + \epsilon_4 \hat{P}_4^{ij}$. Typically, either ϵ_1 or ϵ_0 are the smallest coefficients, such that realizable spin models usually have GSs preferring antiferromagnetic order over ferromagnetic.

9. Conclusions

Summarizing, in the first part of the paper we have analysed the different Mott-insulating phases of repulsive spinor $F = 2$ bosons confined in optical lattices at low temperatures. We have discussed two experimentally relevant cases with either one or two atoms per lattice site. Our analysis shows that in the case of a single atom per lattice site, the spin–spin couplings and, therefore, the magnetic properties of the system can be precisely manipulated using OFR. We have explored the quantum phase diagram for such a case using variational and numerical techniques. On the other hand, the manipulation of the magnetic properties of a GS with two atoms per lattice site becomes much harder to achieve. In this last case, the spin–spin interactions present in the

effective Hamiltonian couple many different virtual states. Since (at zero magnetic field) the scattering lengths a_S are very similar, the couplings depend very strongly on the corresponding Clebsch–Gordan coefficients. In this respect, spinor condensates with non-alkaline atoms [37] which present large differences of their scattering lengths a_S could display stronger spin–spin interactions effects [10]. As it was pointed out to us by L Santos, in the limit when $|t/g_0|$ is very small, the effective spin–spin interactions might involve magnetic dipole–dipole interactions. Still, for rubidium the effective model here is valid for a certain range of $|t/g_0|$ for which the magnetic dipole moment can be neglected. On the other hand, tuning the system into a range where dipole–dipole interactions are important, they might offer an additional knob to control the effective Hamiltonian.

In the second part we have performed a similar analysis of $F = 3/2$ and $5/2$ gases. Also there, while the phases with one fermion (or one fermionic hole, i.e. $2F - 1$ fermions) per lattice site can be more easily controlled with OFR, the physics of phases with 2 or 4 atoms is controlled by the Clebsch–Gordon coefficients. The latter situation might still lead to various spin models preferring either ferromagnetically or antiferromagnetically ordered GSs. In this context it would be particularly appealing to realize (e.g. by the above mentioned dipole–dipole interactions) Hamiltonians with dominant contribution of $\hat{P}_3$-terms. Such Hamiltonians admit AKLT-like gapped GSs in 2D in the honeycomb lattice[9].

Acknowledgments

Appendix A. OFR for $F = 2$ ^{87}Rb atoms

Optical modifications of scattering length, or in other words OFR, were proposed in [46], and carefully analysed theoretically in a series of papers by Bohn and Julienne [59]. These authors have pointed out that OFRs are inevitably associated with spontaneous emission losses, since molecular states used for OFR cannot be to far from the photoassociation resonance. For these reason, changes of natural scattering length of ^{87}Rb, which itself is of order 100 au, by more than 10 au were considered to be unrealistic. These predictions have been confirmed in the recent experiment of Grimm and co-workers [50].

For the present investigations this implies that only limited changes of scattering length are possible. Note that since OFR takes place far from the nucleus, where the excited state potential has a dipole form, $-C_3/R^3$, one can only modify in this way the spin-independent part of the scattering, i.e. $(3a_4 + 4a_2)/7$. This means that a_0 and $4a_4 - 3a_2$ remain unchanged under OFR.

---

[9] We will discuss this particular case in a separate publication.

The most accurate value of $a_2 = (91.28 \pm 0.2)$ au [60]. Bloch and co-workers [61] have studied collisionally driven spin dynamics of ^{87}Rb in MI regime in an optical lattice, and measured very precisely scattering length differences. From these measurements we obtain: $a_0 = 87.77 \pm 0.4$ and $a_4 = 97.23 \pm 0.2$ au. This implies that $4a_4 - 3a_2 = 115.08$ au. Assuming that one may modify spin-independent scattering by 10%, we get $(3a_4 + 4a_2)/7 = 93.83 \pm 9.4$. We see that a_4 may vary roughly as $a_4 = 97.23 \pm 7.9$ au, along the line $4a_4 - 3a_2 = 115.08$ au.

This estimation has important consequences, namely that with OFR it is not feasible to reach the regime $a_4 < a_0$. This is the reason why reaching the regime of a Mott state with two atoms per site and total spin 4 (i.e. $|2, 0, 4\rangle$) is hardly possible with OFRs.

Appendix B. MPS and PEPS: a quantum information approach to strongly correlated systems

The density matrix renormalization group (DMRG)[63, 64] is a variational method that has had an enormous success in describing GSs of some strongly interacting 1D systems with rather modest computational effort. The underlying philosophy of all DMRG-oriented algorithms is that many body systems can be treated almost 'exactly' if one is able to truncate the full Hilbert space by removing the degrees of freedom that are not involved neither in the GS, nor in the dynamical evolution of the system. The difficulty and glory of the method relies on how reliably the truncation is done. Very recently [55, 65, 66, 67], quantum information theory (QIT) has provided a new perspective on the following questions: (i) how to perform an efficient truncation of the Hilbert space, (ii) which quantum systems can be efficiently simulated, (iii) how to simulate dynamical Hamiltonian and dissipative evolutions of strongly correlated systems, (iv) how and when DMRG-oriented methods can be implemented to investigate GSs of 2D and 3D systems; (v) how classical concepts like correlation length, which diverges at the critical points, are linked to entanglement [68], etc.

In perhaps the simplest version, the QIT approach reduces to variational methods based on MPS (in 1D), or, more general, on projected entangled pair states (PEPS). In one dimension, we assume a physical space with tensor product structure $\mathcal{H} = \mathcal{H}_s^{\otimes N}$, where $\mathcal{H}_s$ is the Hilbert space for a single site. We denote a basis on site k by $\{|s_k\rangle, s_k = 1 \ldots \dim \mathcal{H}_s\}$. On each site a virtual Hilbert space $\mathcal{H}_v \equiv \mathcal{H}_d \otimes \mathcal{H}_d$ of two spin-d is introduced, where $\dim \mathcal{H}_d = d \geqslant 1$. In this virtual space, we construct a state $|v\rangle$ formed from maximally entangled pairs of spins on each bond:

$$|v\rangle = \sum_{\alpha_1, \beta_1, \ldots, \alpha_N, \beta_N = 1}^{d} \delta_{\beta_1, \alpha_2} \delta_{\beta_2, \alpha_3} \ldots \delta_{\beta_N, \alpha_1} |\alpha_1, \beta_1\rangle_1 |\alpha_2, \beta_2\rangle_2 \ldots |\alpha_N, \beta_N\rangle \qquad \text{(B.1)}$$

(omitting a normalization constant). Then the space of MPS of size d is defined by

$$\text{MPS}_d := \left\{ \prod_k \hat{A}_k |v\rangle \right\}, \qquad \text{(B.2)}$$

where

$$\hat{A}_k = \sum_{\alpha_k, \beta_k, s_k} (A_k)_{\alpha_k, \beta_k}^{s_k} |s_k\rangle_k \langle \alpha_k, \beta_k| \qquad \text{(B.3)}$$

are projectors to the physical space parametrized by matrices $(A_k)^{s_k} \in \mathbb{C}^{d \times d}$. Evaluating expression (B.2), we find

$$\text{MPS}_d = \left\{ \sum_{s_1, \ldots, s_N} \text{tr}[(A_1)^{s_1} \ldots (A_N)^{s_N}] | s_1, \ldots, s_N \rangle, (A_k)^{s_k} \in \mathbb{C}^{d \times d} \right\}. \qquad \text{(B.4)}$$

The MPS_d form a hierarchy of variational spaces, $\text{MPS}_1 \subset \text{MPS}_2 \subset \ldots$, and allow to efficiently represent 1D many-body states. From the construction through maximally entangled states of Schmidt number d, it is obvious that the value of d necessary to exactly represent a state depends on its amount of entanglement. For the special case of a translationally invariant state, we have $A_1 = A_2 = \ldots = A_N \equiv A$, and thus

$$\text{MPS}_d = \left\{ \sum_{s_1, \ldots, s_N} \text{tr} (A^{s_1} \ldots A^{s_N}) | s_1, \ldots, s_N \rangle, A^{s_k} \in \mathbb{C}^{d \times d} \right\}. \qquad \text{(B.5)}$$

These constructions can be generalized to higher dimensions. In the case of a 2D square lattice, where each sites is connected via four bonds to its nearest neighbours, $\mathcal{H}_v \equiv \mathcal{H}_d^{\otimes 4}$, and $|v\rangle$ is a product of maximally entangled states, one for each bond. Correspondingly, the matrices $(A_k)^{s_k}$ now have four indices, and the contractions are over pairs of indices corresponding to the same bond.

In general, these QIT approaches, apart from being extremely simple to implement, are very efficient for strongly correlated systems and they have already helped to improve our understanding of many body physics. Among recent successes of the QIT approach are: efficient codes for periodic boundary conditions [55], simulations of finite T and dissipative systems [69], renormalization algorithms for quantum many-body systems in two and higher dimensions [54], the understanding of the role of entanglement in quantum phase transitions [68], the efficient evaluation of partition functions of frustrated and inhomogeneous spin systems [70] and of spectra of excited states [23], studies of quantum impurity models [71], simulation of critical [72], and infinite-size [73] quantum lattice systems in 1D, MPS representations of Laughlin wavefunctions [74], simulations of the quantum adiabatic approach to NP-hard problems [75], and MPS based image compression [76], just to name a few.

References

[1] Ho T-L 1998 *Phys. Rev. Lett.* **81** 742
[2] Ohmi T and Machida K 1998 *J. Phys. Soc. Japan* **67** 1822
    Isoshima T, Machida K and Ohmi T 1999 *Phys. Rev.* A **60** 4857
[3] Stenger J, Inouye S, Stamper-Kurn D M, Miesner H J, Chikkatur A P and Ketterle W 1998 *Nature* **396** 345
[4] Schmaljohann H, Erhard M, Kronjager J, Kottke M, van Staa S, Cacciapuoti L, Arlt J J, Bongs K and Sengstock K 2004 *Phys. Rev. Lett.* **92** 040402
[5] Chang M S, Hamley C D, Barrett M D, Sauer J A, Fortier K M, Zhang W, You L and Chapman M S 2004 *Phys. Rev. Lett.* **92** 140403
[6] Barrett M, Sauer J and Chapman M S 2001 *Phys. Rev. Lett.* **87** 010404
[7] Kuwamoto T, Araki K, Eno T and Hirano T 2004 *Phys. Rev.* A **69** 063604

[8] Yi S, Müstecaplioglu Ö E, Sun C P and You L 2002 *Phys. Rev.* A **66** 011601 (R)
Zhang W, Zhou D L, Chang M-S, Chapman M S and You L 2005 *Phys. Rev.* A **72** 013602
Zhang W, Zhou D L, Chang M-S, Chapman M S and You L 2005 *Phys. Rev. Lett.* **95** 180403
Mur-Petit J, Guilleumas M, Polls A, Sanpera A, Lewenstein M, Bongs K and Sengstock K 2006 *Phys. Rev.* A **73** 013629
Moreno-Cardoner M, Mur-Petit J, Guilleumas M, Polls A, Sanpera A and Lewenstein M 2006 *Preprint* cond-mat/0611379
[9] Zhou F 2001 *Phys. Rev. Lett.* **87** 080401
Murkereje S, Xu C and Moore J E 2006 *Phys. Rev. Lett.* **97** 120406
[10] Diener R B and Ho T-L 2006 *Phys. Rev. Lett.* **96** 190405
Santos L and Pfau T 2006 *Phys. Rev. Lett.* **96** 190404
[11] Sengstock K and Bloch I 2006 private communication
[12] Lewenstein M, Sanpera A, Ahufinger V, Damski B, Sen De A and Sen U 2007 *Adv. Phys.* at press (*Preprint* cond-mat/0606771)
[13] Eckert K, Zawitkowski L, Sanpera A, Lewenstein M and Polzik E 2007 *Phys. Rev. Lett.* **98** 100404
[14] Cherng R W and Demler E 2007 *New J. Phys.* **9** 7
[15] Demler E and Zhou F 2002 *Phys. Rev. Lett.* **88** 163001
Imambekov A, Lukin M and Demler E 2003 *Phys. Rev.* A **68** 063602
[16] Yip S K 2003 *Phys. Rev. Lett.* **90** 250402
[17] Auerbach A 1994 *Interacting Electrons and Quantum Magnetism* (New York: Springer)
[18] Yip S K 2003 *J. Phys.: Condens. Matter* **15** 4583
[19] Zhou F 2003 *Europhys. Lett.* **63** 505
[20] Zhou F and Snoek M 2003 *Ann. Phys. (NY)* **308** 692
[21] Zhou F and Snoek M 2004 *Phys. Rev.* B **69** 094410
[22] Rizzi M, Rossini D, De Chiara G, Montangero S and Fazio R 2005 *Phys Rev. Lett.* **95** 240404
[23] Porras D, Verstraete F and Cirac J I 2006 *Phys. Rev.* B **73** 014410
[24] Ciobanu C V, Yip S K and Ho T-L 2001 *Phys. Rev.* A **61** 033607
[25] Koashi M and Ueda M 2000 *Phys. Rev. Lett.* **84** 1066
[26] Ueda M and Koashi M 2002 *Phys. Rev.* A **65** 063602
[27] Ho T L and Yip S K 2000 *Phys. Rev. Lett.* **84** 4031
[28] Barnett R, Turner A and Demler E 2006 *Phys. Rev. Lett.* **97** 180412
[29] Zhou F and Semenoff G W 2006 *Phys. Rev. Lett.* **97** 180411
[30] Jaksch D, Bruder C, Cirac J I, Gardiner C W and Zoller P 1998 *Phys. Rev. Lett.* **81** 3108
[31] Hofstetter W, Cirac J I, Zoller P, Demler E and Lukin M D 2005 *Phys. Rev. Lett.* **89** 220407
[32] Paananen T, Martikainen J-P and Torma P 2006 *Phys. Rev.* A **73** 053606
[33] Liu W V, Wilczek F and Zoller P 2004 *Phys. Rev.* A **70** 033603
[34] Hofstetter W 2005 *Adv. Solid State Phys.* **45** 109
[35] Weber T, Herbig J, Mark M, Nagerl H C and Grimm R 2003 *Science* **299** 232
[36] Takahashi Y, Takasu Y, Maki K, Komori K, Takano T, Honda K, Yamaguchi A, Kato Y, Mizoguchi M, Kumakura M and Yabuzaki T 2004 *Laser Phys.* **14** 621
[37] Griesmaier A, Werner J, Hensler S, Stuhler J and Pfau T 2005 *Phys. Rev. Lett.* **94** 160401
[38] Wu C, Hu J-P and Zhang S-C 2003 *Phys. Rev. Lett.* **91** 186402
[39] Wu C 2005 *Phys. Rev. Lett.* **95** 266404
[40] Wu C, Hu J-P and Zhang S-C 2005 *Phys. Rev. Lett.* submitted (*Preprint* cond-mat/0512602)
[41] Lecheminant P, Boulat E and Azaria P 2005 *Phys. Rev. Lett.* **95** 240402
[42] Capponi S, Roux G, Azaria P, Boulat E and Lecheminant P 2007 *Phys. Rev.* B **75** 100503 (*Preprint* cond-mat/0612456)
[43] Controzzi D and Tsvelik A M 2006 *Phys. Rev. Lett.* **96** 097205
[44] Wu C 2006 *Mod. Phys. Lett.* B **20** 1707

IOP Institute of Physics ⬤ DEUTSCHE PHYSIKALISCHE GESELLSCHAFT

[45] Timmermans E, Tommasini P, Hussein M and Kerman A 1999 *Phys. Rep.* **315** 199

[46] Fedichev P O, Kagan Y, Shlyapnikov G V and Walraven J T M 1996 *Phys. Rev. Lett* **77** 2913

[47] Fannes M, Nachtergaele B and Werner R F 1992 *Commun. Math. Phys.* **144** 441

[48] Affleck I, Kennedy T, Lieb E H and Tasaki H 1987 *Phys. Rev. Lett.* **59** 799

[49] Eckert K, Zawitkowski Ł, Leskinen M J, Sanpera A and Lewenstein M 2006 *Preprint* cond-mat/0603273

[50] Theis M, Thalhammer G, Winkler K, Hellwig M, Ruff G, Grimm R and Hecker Denschlag J 2004 *Phys. Rev. Lett.* **93** 123001

[51] Cornish S L, Claussen N R, Roberts J L, Cornell E A and Wieman C E 2000 *Phys. Rev. Lett.* **85** 1795

[52] Alet F, Walczak A M and Fisher M P A 2006 *Physica* A **369** 122

[53] Wolf M M, Ortiz G, Verstraete F and Cirac J I 2006 *Phys. Rev. Lett.* **97** 110403

[54] Verstraete F and Cirac J I 2004 *Preprint* cond-mat/0407066
Murg V, Verstraete F and Cirac J I 2007 *Phys. Rev. A* **75** 033605 (*Preprint* cond-mat/0611522)
Jordan J, Orus R, Vidal G, Verstraete F and Cirac J I 2007 *Preprint* cond-mat/0703788

[55] Verstraete F, Porras D and Cirac J I 2004 *Phys. Rev. Lett.* **93** 227205

[56] Tu H-H, Yu G-M and Yu L 2006 *Phys. Rev.* B **74** 174404

[57] Chen S, Wu C, Zhang S-C and Wang Y 2005 *Phys. Rev.* B **72** 214428

[58] Sutherland B 1975 *Phys. Rev.* B **12** 3795

[59] Kennedy T, Lieb E H and Tasaki H 1988 *J. Stat. Mech.* **53** 1019

[60] Bohn J L and Julienne P S 1997 *Phys. Rev. A* **56** 1486
Bohn J L and Julienne P S 1999 *Phys. Rev. A* **60** 414

[61] van Kampen E G M, Kokkelmans S J J M F, Heinzen D J and Verhaar B J 2002 *Phys. Rev. Lett.* **88** 093201

[62] Widera A, Gerbier F, Folling S, Gericke T, Mandel O and Bloch I 2006 *New J. Phys.* **8** 152 (*Preprint* cond-mat/0604038)

[63] White S R 1992 *Phys. Rev. Lett.* **69** 2863

[64] Schollwöck U 2005 *Rev. Mod. Phys.* **77** 259

[65] Vidal G 2003 *Phys. Rev. Lett.* **91** 147902

[66] Vidal G 2004 *Phys. Rev. Lett.* **93** 040502

[67] Orús R and Lattore J I 2004 *Phys. Rev. A* **69** 052308

[68] Verstraete F, Popp M and Cirac J I 2004 *Phys. Rev. Lett.* **92** 027901
Vidal G, Latorre J I, Rico E and Kitaev A 2003 *Phys. Rev. Lett.* **90** 227902

[69] Verstraete F, Martín-Delgado M A and Cirac J I 2004 *Phys. Rev. Lett.* **92** 087201

[70] Murg V, Verstraete F and Cirac J I 2005 *Phys. Rev. Lett.* **95** 057206

[71] Verstraete F, Weichselbaum A, Schollwock U, Cirac J I and von Delft J 2005 *Preprint* cond-mat/0504305

[72] Vidal G 2005 *Preprint* cond-mat/0512165

[73] Vidal G 2007 *Phys. Rev. Lett.* **98** 070201 (*Preprint* cond-mat/0605597)

[74] Iblisdir S, Latorre J I and Orús R 2007 *Phys. Rev. Lett.* **98** 060402 (*Preprint* cond-mat/0609088)

[75] Latorre J I 2005 *Preprint* quant-ph/0510031

[76] Banuls M C, Orús R, Latorre J I, Perez A and Ruiz-Femenia P 2006 *Phys. Rev. A* **73** 022344